

Second-order and Fluctuation-induced First-order Phase Transitions with Functional Renormalization Group Equations

Kenji Fukushima

Department of Physics, Keio University, Kanagawa 223-8522, Japan

Kazuhiko Kamikado

Yukawa Institute for Theoretical Physics, Kyoto University, Kyoto 606-8502, Japan

Bertram Klein

Technische Universität München, James-Frank-Strasse 1, 85748 Garching, Germany

We investigate phase transitions in scalar field theories using the functional renormalization group (RG) equation. We analyze a system with $U(2) \times U(2)$ symmetry, in which there is a parameter λ_2 that controls the strength of the first-order phase transition driven by fluctuations. In the limit of $\lambda_2 \rightarrow 0$, the $U(2) \times U(2)$ theory is reduced to an $O(8)$ scalar theory that exhibits a second-order phase transition in three dimensions. We develop a new insight for the understanding of the fluctuation-induced first-order phase transition as a smooth continuation from the standard RG flow in the $O(8)$ system. In our view from the RG flow diagram on coupling parameter space, the region that favors the first-order transition emerges from the unphysical region to the physical one as λ_2 increases from zero. We give this interpretation based on the Taylor expansion of the functional RG equations up to the fourth order in terms of the field, which encompasses the ε -expansion results. We compare results from the expansion and from the full numerical calculation and find that the fourth-order expansion is only of qualitative use and that the sixth-order expansion improves the quantitative agreement.

PACS numbers: 64.60.ae, 11.30.Rd, 12.38.Aw, 12.38.Lg

I. INTRODUCTION

Phase transitions occur in many different physical systems. In this paper we shall address a fluctuation-induced first-order phase transition or the Coleman-Weinberg potential [1–11] in the system with $U(2) \times U(2)$ symmetry, as well as a second-order one in the system with $O(8)$ symmetry [12–24] as a particular limit of the $U(2) \times U(2)$ theory. This particular choice of the global symmetries is motivated by those relevant for phase transitions in the strong interactions.

The fundamental theory of the strong interactions is Quantum Chromodynamics (QCD), which describes the dynamics of quarks and gluons. It is known that at a temperature T of the same order as the typical QCD scale, Λ_{QCD} , QCD undergoes two types of phase transitions — the chiral phase transition and the quark deconfinement transition [25]. In particular at the chiral phase transition the behavior of the system should be characterized by global chiral symmetry [7, 26].

For N_f flavors of massless quarks the QCD Lagrangian is invariant under a flavor rotation of the $U(N_f)_L \times U(N_f)_R$ symmetry for left- and right-handed quarks. Because of the axial anomaly, the subgroup $U(1)_A$ is explicitly broken (down to Z_{2N_f}) on the quantum level, so that in this case the (continuous) symmetry is reduced to $SU(N_f)_L \times SU(N_f)_R \times U(1)_V$. Here, the vector symmetry $U(1)_V$ corresponds to the conserved baryon charge and is not broken in the normal phase.

In the QCD vacuum chiral symmetry is spontaneously broken by a nonzero chiral condensate [27] according to

$SU(N_f)_L \times SU(N_f)_R \rightarrow SU(N_f)_V$. In the two-flavor case the symmetry breaking pattern, $SU(2)_L \times SU(2)_R \rightarrow SU(2)_V$, is equivalent to $SO(4) \rightarrow SO(3)$, and hence can be mapped onto a (scalar) meson model with $O(4)$ symmetry [28]. This provides a motivation to investigate phase transitions of the $O(N)$ scalar theory in the finite- T formalism in $d = 4$ dimensions, or in the zero- T formalism in $d = 3$ dimensions, if we assume that the critical behavior is described with a dimensionally reduced theory [29]. In this paper we address the Renormalization Group (RG) flow of the theory in the dimensionally reduced description only. This can be justified as follows: At finite temperature, the Euclidean time direction in a d -dimensional path-integral description becomes compactified. Because of this finite extent in the Euclidean time direction, in a region close enough to a critical point, the dominant long-range fluctuations will be unable to propagate in the time direction and the system will in effect become $(d - 1)$ dimensional. For a finite- T theory in $d = 4$ space-time it is therefore expected that the critical behavior can be described in terms of an effective $d = 3$ dimensional theory at $T = 0$ with its couplings (which are T -dependent) set close to their critical values.

In contrast to the situation described above, if the axial symmetry is *effectively* restored close to the transition temperature (e.g. because of the instanton suppression at high T [30–32]), the relevant symmetry for the $N_f = 2$ transition is then $U(2)_L \times U(2)_R$, which leads us to the analysis on the $U(2) \times U(2)$ scalar theory.

Assuming that a particular phase transition is of second order and displays critical behavior, one can rely on

universality arguments to describe the system in terms of an effective Landau-Ginzburg-Wilson functional which is determined solely from the symmetries and the dimensionality of the system. The description in terms of such an effective theory is often much simpler than the original microscopic theories, but still captures the long-range phenomena at the critical point.

In the investigation of critical phenomena, the correct treatment of low-momentum modes is of paramount importance. Close to a critical point, physical properties of a system are dominated by these low-lying soft modes. Since the system has no intrinsic length scale at the critical point, phenomena on all length scales contribute and non-trivial anomalous dimensions can appear. In the case of scalar theories, the anomalous dimension at the critical point is generally small, which can justify a simplified treatment.

Renormalization group methods have been used to deal with the infrared (IR) divergences which appear in the vicinity of critical points [33]. Historically speaking, the ε -expansion around $d = 4$ dimensions for theories with upper critical dimension $d = 4$ has been of great importance [34, 35]. While the RG methods are able to deal with IR divergences, calculations of this type are still perturbative and rely on an additional expansion in terms of small coupling constants, which can be justified by the fact that the coupling constants are of order of ε in the vicinity of the fixed points. There is a countless number of works on the application of RG methods to the second-order phase transition in the $O(N)$ theory [7, 18–24].

On the other hand, the theory with $U(2) \times U(2)$ -symmetry requires more investigation. In the context of the chiral phase transition in QCD, such an effective theory has been extensively discussed by Pisarski and Wilczek [5, 7, 26]. In their results the ε -expansion analysis does not find an IR stable fixed point which could control a continuous transition. This indicates that the transition is presumably driven by fluctuations to be of first order. [See also [3, 9, 36]].

This question of the order of the chiral phase transition including the possibility of the effective $U(1)_A$ symmetry restoration has been further analyzed in and beyond the ε -expansion in e.g. [37–39] using field-theoretical methods and in [40–43] using functional RG methods [44–46] as well as the finite- T lattice-QCD simulation [47]. Closely related first-order phase-transitions have been investigated in [9–11, 48] with the functional RG. In a gauge theory setting, the functional RG has been used to estimate effects of the anomaly on chiral symmetry breaking [49] and on the phase transition line [50] in QCD. Also, anomaly effects on the mass spectrum have been described in [51] by means of non-perturbative Dyson-Schwinger equations.

The functional RG approach does not rely on an expansion in terms of a small coupling and is capable of describing the full effective potential. This enables us to directly analyze the critical behavior associated with not

only the second-order but also first-order phase transitions. For reviews of the method see e.g. [45, 46, 52–60].

We use a functional RG equation to describe the behavior of the $U(2) \times U(2)$ matrix model at the fluctuation-induced first-order phase transition in the same way as done by Berges and Wetterich [42]. We establish the connection between the functional RG flow equations in the formulation according to [44] (i.e. the Wetterich equation) and the ε -expansion. While there is some literature on the connection between the functional RG and perturbative calculations [9, 22, 61, 62], this connection we address is a useful starting point to explore the general RG flow diagram. Moreover, to our knowledge, nobody has explicitly retrieved the ε -expansion results from the Wetterich equation for the $U(2) \times U(2)$ system. [See also [36, 63]. The connection of the ε -expansion to functional RG equations in a related formalism and the emergence of the Wilson-Fisher fixed-point in this approach have been pointed out in [60].]

Since we are motivated by an interest in the QCD phase transition at finite temperature, we will adhere to the QCD terminology throughout this paper. That is, we will refer to the 8-component fields in the $O(8)$ and $U(2) \times U(2)$ theory as the σ -field for the condensing mode which acquires a non-zero expectation value and as the $\vec{\pi}$ -fields for the 3 pseudo-scalar components that are Nambu-Goldstone bosons. These 4 mesons have parity partners, namely, η -field and \vec{a}_0 -fields. Apart from this, nevertheless, our treatment is generic and is completely parallel to the earlier works by Berges and Wetterich [42] and by Berges, Tetradis, and Wetterich [43]. In the next section, as a convenience to readers, we will briefly summarize our aims in this paper and discuss where they advance beyond those earlier works.

We intend the current calculation as a starting point for further investigations of the transition in the framework of more realistic phenomenological models for QCD thermodynamics [64–72]. In such models gauge degrees of freedom can also be taken into account, but the possibility of a fluctuation-induced change of the order of the transition has not yet been fully investigated due to technical complexity. The inclusion of such effects beyond the mean-field level in these models would be a very interesting problem in the future.

We will organize this paper as follows: We first present a summary of our central results in Sec. II. Then we make a quick review over the functional RG formalism in Sec. III. We discuss the analytical and numerical calculations in great details in Sec. IV. Section V contains our concluding remarks.

II. CENTRAL RESULTS

The phase transitions of the $U(2) \times U(2)$ scalar theory have been extensively studied in earlier works in the functional RG formalism [42, 43]. Although there are minor differences in the technical setup, we have performed nu-

merical calculations at the same level of approximation and truncation as used by Berges, Tetradis, and Wetterich in [42, 43]. Before we discuss the details of the calculation, we therefore wish to point out the qualitatively new aspects of this work.

First of all, we would like to emphasize that we use a very simple form of the flow equations (given by Eqs. (39) and (43) below) in the local potential approximation which does no longer involve momentum integrations. This difference from the equations in [42, 43] arises from a different choice of the IR regulator function. Apart from the wave-function renormalization, which we neglect, the information contained in the RG flow equation is equivalent. Since the content is equivalent, the simpler expressions are advantageous, both for an analysis of the structure of the RG flow and for numerical calculations. In fact, as we will demonstrate explicitly later in the discussion, we can reproduce the result from the ε -expansion in a short calculation of only a few lines and make the connection between the functional RG equation and the perturbative method very transparent. This is certainly not a qualitative breakthrough, but such a technical improvement provides useful progress for practical calculations.

Second, in this work we propose a new point of view for understanding the fluctuation-induced first-order phase transition. If the phase transition is of second order, the flow diagram and the fixed-point structure can be studied very well in the space of the coupling parameters. For instance, in the case of the $O(N)$ scalar theory in three dimensions with a field $\phi = (\phi_1, \dots, \phi_N)^T$, the relevant operators in terms of the squared field $\varphi = \phi^2$ are φ and φ^2 . The (IR-scale dependent) effective potential can thus be written as

$$U_k(\varphi) = \frac{1}{2}\mu_k^2\varphi + \frac{1}{4!}\lambda_{1k}\varphi^2. \quad (1)$$

The relevant coupling parameters, μ_k^2 and λ_{1k} , run as the IR scale k becomes smaller and fluctuations are integrated out. Using dimensionless variables $\bar{\mu}_k^2 \equiv k^{-2}\mu_k^2$ and $\bar{\lambda}_{1k} = k^{-1}\lambda_{1k}$, we obtain Fig. 1. Starting from a set of differential flow equations to be derived later, the figure shows how these dimensionless couplings change under a change of the scale k .

The interpretation of such a RG-flow diagram is merely textbook knowledge. We sketch an illustration in Fig. 2 to extract the essential features from Fig. 1. If the flow goes toward the left side to smaller values of $\bar{\mu}_k^2$, the symmetric state at $\varphi = 0$ becomes more and more unstable and the system falls into the symmetry-broken phase with $\varphi \neq 0$. If the flow goes in the opposite direction toward the right to larger values of $\bar{\mu}_k^2$, on the other hand, the symmetric phase is a stable ground state. Therefore there is a critical line separating these two regimes. If the flow starts on the critical line, the system approaches the IR fixed-point which is the critical point characterizing the phase transition.

In the shaded region in Fig. 2 the flow goes deeper into the region with $\bar{\mu}_0^2 > 0$ and $\bar{\lambda}_{10} < 0$. Usually such

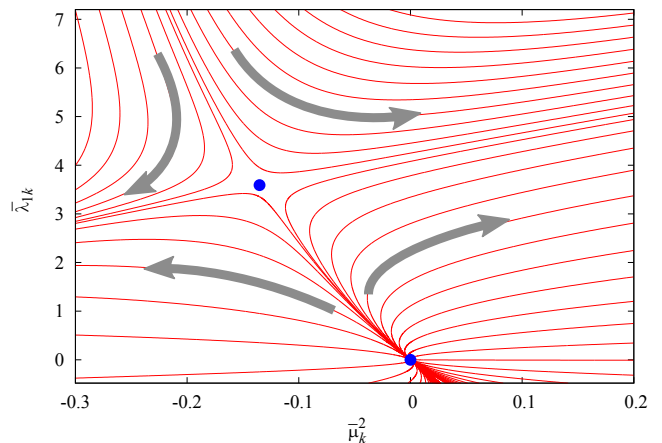


FIG. 1. RG flow diagram in the $\bar{\mu}_k^2$ - $\bar{\lambda}_{1k}$ plane for the $d = 3$ $O(8)$ scalar theory that is realized from the $U(2) \times U(2)$ theory with $\bar{\lambda}_{2\Lambda} = 0$ chosen initially. The arrows indicate the direction from larger to smaller k and the dots represent the fixed points.

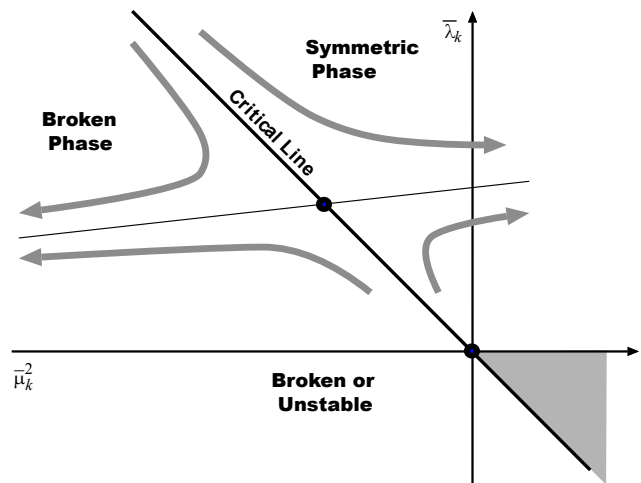


FIG. 2. General structure of the RG flow for the $d = 3$ $O(N)$ scalar theory. In the shaded region the flow goes to $\bar{\mu}_0^2 > 0$ and $\bar{\lambda}_{10} < 0$ that is the “necessary condition” for a double-well shape in the effective potential (1).

flow patterns are physically meaningless in the analysis of the $O(N)$ theory because negative λ_{10} makes the potential (1) unbounded and the theory is not well defined there. Nevertheless, from the interest in the first-order transition, this shaded region is interesting. This is because, in view of the potential form (1), the destination of the flow, $\bar{\mu}_0^2 > 0$ and $\bar{\lambda}_{10} < 0$, is just the “necessary condition” to realize a double-well shape (see Fig. 3). Of course this is not a “sufficient condition” and the existence of the double-well shape depends on how large the sixth-order coupling constant ζ_1 associated with φ^3 is (see Eq. (45)). If ζ_1 is too small, the potential is not stabilized until very large values of φ have been reached, for which an expansion like Eq. (1) is unsuitable. If ζ_1 is too large, the second minimum at $\varphi \neq 0$ simply vanishes

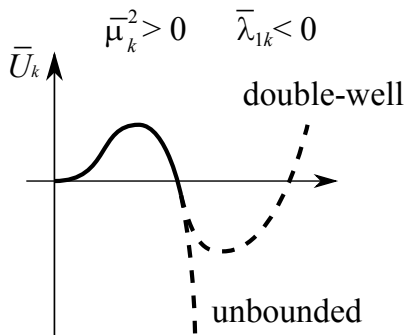


FIG. 3. Potential shape for $\bar{\mu}_k^2 > 0$ and $\bar{\lambda}_{1k} < 0$. Depending on the sixth-order coefficient the potential may take a double-well form.

and the symmetric phase is always the most stable. Nevertheless, we can say that, if there is a region where the first-order phase transition exists, the flow must satisfy the necessary condition, meaning that the flow must be headed for the region with $\bar{\mu}_0^2 > 0$ and $\bar{\lambda}_{10} < 0$.

The $U(2) \times U(2)$ theory has at least one more coupling constant λ_2 in addition to μ^2 and λ_1 (and ζ_1) as defined in Sec. IV. For $\lambda_2 = 0$ the theory is reduced into the $O(8)$ scalar theory. Then, recalling the discussions in the previous paragraph, we can formulate our expectations about the evolution of the phase diagram.

An interesting question is the following: How does the RG-flow diagram or more specifically the shaded region in Fig. 2 change in the $U(2) \times U(2)$ model as the additional coupling λ_2 increases from zero? This question does not seem to have been answered explicitly in the earlier works by Berges, Tetradis, and Wetterich [42, 43] nor by Alford and March-Russell [9], though those works contain extensive and detailed discussions.

Answering this question is quite intriguing because, as we have explained above, the shaded region has a direct connection to the emergence of the double-well shape in the effective potential. We can understand the results in a way parallel to the $O(8)$ case, using the phase diagram in space spanned by $\bar{\mu}_k^2$ and $\bar{\lambda}_{1k}$. Primarily this is just a replacement of the variables used to draw the phase diagram, but it also provides a useful interpretation in terms of the shape of the potential and we believe that it is worth taking a closer look at this interpretation in the following.

Before we discuss the results shown in Figs. 4, 5, and 6, we remark that the horizontal and vertical axes are not, strictly speaking, identical to those in the previous Fig. 1. In the diagram we use $\bar{\mu}_\Lambda^2$ and $\bar{\lambda}_{1\Lambda}$, which are the coupling parameters at the UV scale $k = \Lambda$, to show the shaded regions. If the flow starts with initial $\bar{\mu}_\Lambda^2$ and $\bar{\lambda}_{1\Lambda}$ inside the shaded region and the specified $\bar{\lambda}_{2\Lambda}$ for each figure, it goes toward $\bar{\mu}_0^2 > 0$ and $\bar{\lambda}_{10} < 0$ at the IR scale $k \approx 0$. In the numerical calculation, we do not actually take the limit of $k \rightarrow 0$ but stop the flow at $k/\Lambda = 0.1$. This is a prescription for the numerical calculation (i.e. the choice of 0.1 is just arbitrary). As

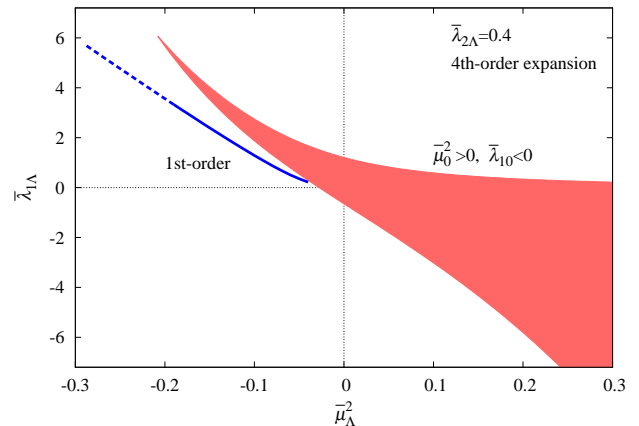


FIG. 4. Initial condition region at the UV scale necessary for the double-well shape in the effective potential at the IR scale. Results are from the fourth-order Taylor expansion. The line labelled with “1st-order” represents the phase transition points of fluctuation-induced first order as a result of full numerical evaluation in the grid method.

discussed in [9, 42, 43], in the context of a first-order transition with bubble formation, it would make physical sense to stop the flow at some point whose scale should be related to the bubble thickness.

The RG-flow diagram for the $U(2) \times U(2)$ model similar to Fig. 1 is available from the solution of the RG equations for the coupling parameters, that is, the Taylor expansion coefficients. In the same way as for the $O(N)$ model we have performed the Taylor expansion for the $U(2) \times U(2)$ system to derive a set of partial differential equations for $\bar{\mu}_k^2$, $\bar{\lambda}_{1k}$, and $\bar{\lambda}_{2k}$. Then, solving the differential equations numerically, we have identified the shaded region corresponding to that in Fig. 2 in the $O(N)$ theory.

Figure 4 shows the results from the Taylor expansion up to the fourth order in terms of the field (or the second order in terms of $\varphi = \phi^2$). It is clear that our expectation is manifestly fulfilled: The shaded region is elongated from the unphysical region in the $O(N)$ case and spreads almost along the critical line toward the physical region at $\bar{\mu}_\Lambda^2 < 0$ and $\bar{\lambda}_{1\Lambda} > 0$.

As we will describe in detail in a later section, we have carried out a full numerical calculation without resorting to an expansion by putting the function $U_k(\varphi)$ on a grid of discretized field values. In this way we can confirm the double-well potential form already reported in the earlier works by Berges, Tetradis, and Wetterich [42, 43]. While our method does not surpass the earlier works in precision, we use a regulator that leads to much simpler flow equations.

The line labelled with “1st-order” in Fig. 4 represents the phase transition points of fluctuation-induced first order. The strength of the first-order transition weakens with decreasing $\bar{\mu}_\Lambda^2$ and eventually it becomes smaller than the resolution in the grid method. We indicate this

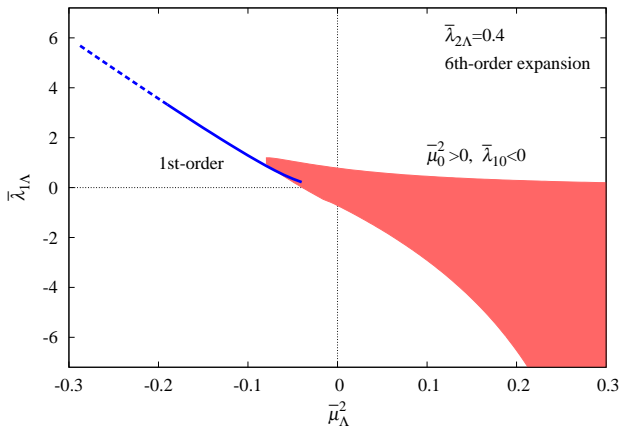


FIG. 5. The shaded region indicates the initial conditions at the UV scale necessary to obtain the double-well shape in the effective potential at the IR scale. Results are from the sixth-order Taylor expansion for $\bar{\lambda}_{2\Lambda} = 0.4$.

by changing the solid line to a dotted one. We can see that the agreement between the results from the fourth-order Taylor expansion and from the full numerical evaluation is limited to a qualitative level. Guided by the expectation that the agreement would be better, we have investigated the phase diagram from the sixth-order Taylor expansion.

We show the results from the sixth-order Taylor expansion in Fig. 5. The phase transition line seems to be smoothly connected to the shaded region in this case. The agreement is, however, not as good as we expected. [We have checked that the second minimum in the potential lies in the region where φ is sufficiently smaller than unity in all the cases, so that the Taylor expansion should work in principle.] We will discuss the quantitative comparison for the shape of the potential with and without expansion later.

So far, we have seen the results for a fixed choice of $\bar{\lambda}_{2\Lambda} = 0.4$. According to [42, 43], the first-order phase transition is strengthened with increasing $\bar{\lambda}_{2\Lambda}$. We can reconfirm this observation by repeating the calculations for larger $\bar{\lambda}_{2\Lambda}$. Figure 6 shows the results for a larger choice of $\bar{\lambda}_{2\Lambda} = 0.7$. We can see that the shaded region in Fig. 6 becomes slightly wider than that in Fig. 5. Also the dotted line disappears since the first-order phase transition becomes more prominent and is resolved by the grid in the region shown.

If we choose even larger values of $\bar{\lambda}_{2\Lambda}$, we find that the shaded region is pulled not along the critical line, but upward toward larger values of $\bar{\mu}_\Lambda^2$, while the position of the first-order transition line hardly moves.

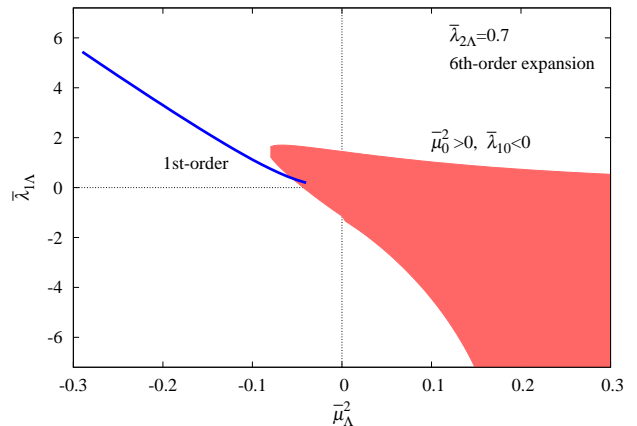


FIG. 6. The shaded region indicates the initial conditions at the UV scale necessary to obtain the double-well shape in the effective potential at the IR scale. Results are from the sixth-order Taylor expansion for $\bar{\lambda}_{2\Lambda} = 0.7$.

III. FORMALISM

To make our discussion as self-contained as possible, we shall briefly review the functional RG formalism and the equations we are using in this paper. The functional RG is an exact formulation of quantum field theories in the form of a functional differential equation [44–46]. In the formulation we are using, the central object is the effective action which is calculated non-perturbatively. In the functional RG one defines an average effective action with the IR-cutoff scale k . For a general scalar field χ whose classical counterpart is denoted by $\phi = \langle \chi \rangle$ here, the k -dependent effective action is defined by

$$\Gamma_k[\phi] = -\log \left[\int [d\chi] \exp \left(-S[\chi] - \Delta S_k[\chi - \phi] + \int d^d x \frac{\delta \Gamma_k[\phi]}{\delta \phi(x)} [\chi(x) - \phi(x)] \right) \right], \quad (2)$$

where the IR-cutoff dependence is introduced by a mass-like term,

$$\Delta S_k = \frac{1}{2} \int \frac{d^d q}{(2\pi)^d} R_k(q) \phi(-q) \phi(q) \quad (3)$$

in momentum space. Here we consider d -dimensional space-time generally. We note that the momentum-dependent mass $R_k(q)$ should cut off IR modes with $q < k$. That is, $R_k(q)$ must satisfy the following requirement [44–46]; soft modes with $q \ll k$ should be quenched by large $R_k(q) \sim k^2$, while $R_k(q) \sim 0$ for $q \gg k$. Equation (2) together with the properties of $R_k(q)$ leads to the boundary condition for the average effective action; $\Gamma_\Lambda[\phi] = S[\phi]$ where Λ is the UV scale where the RG flow starts, and $\Gamma_0[\phi] = \Gamma[\phi]$ where $\Gamma[\phi]$ is the full effective action defined in the textbook manner. In principle, the IR-cutoff function can be arbitrary as long as it satisfies

the above-mentioned properties. In this paper we make use of the ‘‘optimized’’ choice of $R_k(q)$ [56, 73, 74] proposed by Litim [74],

$$R_k(q) = (k^2 - q^2)\theta(k^2 - q^2), \quad (4)$$

where q refers to a d -dimensional vector in Euclidean space-time and θ is the Heaviside step function. The choice of a cutoff function is in general not unique, but the optimized choice [74] ensures the correct universal behavior [75]. (For finite- T studies it is a better choice to use the cutoff for only spatial momenta [76, 77].)

Armed with these definitions, we can reach the functional RG equation (known as the Wetterich equation [44]) by differentiating $\Gamma_k[\phi]$ with respect to k , i.e.

$$\frac{\partial\Gamma_k[\phi]}{\partial k} = \frac{1}{2}\text{Tr}\left[\frac{\partial R_k}{\partial k}\left(\Gamma_k^{(2)}[\phi] + R_k\right)^{-1}\right]. \quad (5)$$

Here Tr means the trace over any intrinsic indices of ϕ as well as the trace over the functional space. In the above $\Gamma_k^{(2)}[\phi]$ denotes the second-order functional derivative of $\Gamma_k[\phi]$ with respect to the field ϕ , and $\Gamma_k^{(2)}[\phi] + R_k$ is thus an inverse of the full propagator including the IR-cutoff term. From this one can acquire an intuitive interpretation for the left-hand side of Eq. (5) as a one-loop integration attached to the cutoff derivative, $\partial R_k/\partial k$. Nevertheless, since the derivation assumes no approximation, Eq. (5) is ‘‘exact’’ and contains full quantum effects.

In practice, however, solving the functional RG equation without any truncation is as difficult as finding an exact solution of the theory. We should thus make an approximation. Here we adopt the local potential approximation (LPA) in which the effective action $\Gamma_k[\phi]$ is assumed to be of the form,

$$\Gamma_k[\phi] = \int d^d x \left(\frac{1}{2} \partial_\mu \phi \partial_\mu \phi + U_k(\phi) \right), \quad (6)$$

in d -dimensional Euclidean space-time. The k -dependent effective potential $U_k(\phi)$ is a local function of the fields. This approach is frequently taken in theories involving only scalar fields and is sufficient as long as the anomalous dimension remains small. Thanks to the particular choice (4) one can easily perform the q -integration after Eq. (6) is substituted for $\Gamma_k[\phi]$ in Eq. (5) (and ϕ is assumed to be spatially constant). Finally the functional RG equation simply reads

$$\frac{\partial U_k}{\partial k} = K_d k^{d+1} \sum_i \frac{1}{E_i^2}. \quad (7)$$

The index i refers to the field components ϕ_i . Here, we have defined $K_d = S_d/(2\pi)^d$ with the volume of a d -dimensional sphere S_d given by

$$S_d = \frac{2\pi^{d/2}}{d\Gamma(d/2)}, \quad (8)$$

that is, for example, for $d = 3$ we need

$$K_3 = \frac{1}{6\pi^2}. \quad (9)$$

The energy in the denominator of Eq. (7) is

$$E_i^2 = k^2 + M_i^2, \quad (10)$$

where M_i denotes the mass eigenvalues of the second-derivative matrices of the effective potential,

$$M_{ij} = \frac{\partial^2 U_k(\phi)}{\partial \phi_i \partial \phi_j}. \quad (11)$$

Although Eq. (7) is very simple, it encompasses rich contents of the critical phenomena, as we will see later.

IV. $U(2) \times U(2)$ SCALAR THEORY

We are now ready to proceed to our main subject, i.e. the fluctuation-induced first-order phase transition. For this purpose we adapt the $U(2) \times U(2)$ scalar theory in $d = 3$ dimensions and introduce some notations according to hadron physics.

A. Notations

We can write the Lagrangian density of the $U(2) \times U(2)$ theory conveniently as [7]

$$\mathcal{L} = \frac{1}{2}\text{tr}[\partial_\mu \Phi \partial^\mu \Phi^\dagger] + \frac{1}{2}\mu^2\text{tr}[\Phi \Phi^\dagger] - g_1(\text{tr}[\Phi \Phi^\dagger])^2 - g_2\text{tr}[\Phi \Phi^\dagger \Phi \Phi^\dagger] \quad (12)$$

with a complex 2×2 matrix Φ . This Lagrangian density is invariant under the transformation,

$$\Phi \longrightarrow V_L \Phi V_R^\dagger, \quad (13)$$

where V_L and V_R^\dagger are independent $U(2)$ matrices. In the context of chiral symmetry of QCD, the matrix Φ has a parametrization in terms of the hadronic degrees of freedom:

$$\Phi = \Sigma + i\Pi = \sum_{a=0}^3 t_a(\sigma_a + i\pi_a), \quad (14)$$

where the t_a are the $u(2)$ generators (and unity) normalized according to $\text{tr}[t_a t_b] = \delta_{ab}$. We can write

$$\Sigma = \begin{pmatrix} \frac{1}{\sqrt{2}}a^0 + \frac{1}{\sqrt{2}}\sigma & & a^+ \\ a^- & & -\frac{1}{\sqrt{2}}a^0 + \frac{1}{\sqrt{2}}\sigma \end{pmatrix}, \quad (15)$$

$$\Pi = \begin{pmatrix} \frac{1}{\sqrt{2}}\pi^0 + \frac{1}{\sqrt{2}}\eta & & \pi^+ \\ \pi^- & & -\frac{1}{\sqrt{2}}\pi^0 + \frac{1}{\sqrt{2}}\eta \end{pmatrix}, \quad (16)$$

using the conventional notation in hadron physics; $a^0 = \sigma_3$, $a^\pm = (a^1 \mp ia^2)/\sqrt{2} = (\sigma_1 \mp i\sigma_2)/\sqrt{2}$, $\sigma = \sigma_0$ for the scalar sector and $\pi^0 = \pi_3$, $\pi^\pm = (\pi^1 \mp i\pi^2)/\sqrt{2} = (\pi_1 \mp i\pi_2)/\sqrt{2}$, $\eta = \pi_0$ for the pseudo-scalar sector. [This η does not correspond to the physical η in nature but to the flavor-singlet η_0 which mixes partially with η_3 to become the physical η' .] With this notation the Lagrangian density in Euclidean space-time is expressed as

$$\mathcal{L} = \partial_\mu \sigma \partial_\mu \sigma + \partial_\mu \vec{\pi} \cdot \partial_\mu \vec{\pi} + \partial_\mu \eta \partial_\mu \eta + \partial_\mu \vec{a} \cdot \partial_\mu \vec{a} + U_\Lambda, \quad (17)$$

where we find the potential,

$$\begin{aligned} U_\Lambda &= \frac{1}{2} \mu_\Lambda^2 (\sigma^2 + \vec{\pi}^2 + \eta^2 + \vec{a}^2) \\ &+ \left(g_1 + \frac{1}{2} g_2 \right) (\sigma^2 + \vec{\pi}^2 + \eta^2 + \vec{a}^2)^2 \\ &+ 2g_2 \left[(\sigma^2 + \vec{\pi}^2)(\eta^2 + \vec{a}^2) - (\sigma\eta + \vec{\pi} \cdot \vec{a})^2 \right], \end{aligned} \quad (18)$$

from Eq. (12). To simplify the notation in what follows, we introduce the new couplings and variables;

$$\lambda_1 \equiv 4! \left(g_1 + \frac{1}{2} g_2 \right), \quad \lambda_2 \equiv 2g_2, \quad (19)$$

$$\begin{aligned} \varphi &\equiv \sigma^2 + \vec{\pi}^2 + \eta^2 + \vec{a}^2, \\ \xi &\equiv (\sigma^2 + \vec{\pi}^2)(\eta^2 + \vec{a}^2) - (\sigma\eta - \vec{\pi} \cdot \vec{a})^2. \end{aligned} \quad (20)$$

Roughly speaking σ plays the role of the component of ϕ that acquires a finite expectation value in the $O(N)$ scalar theory and φ defined above is the counterpart of ϕ^2 . Using these variables we can rewrite Eq. (18) into a concise representation as follows:

$$U_\Lambda(\varphi, \xi) = \frac{1}{2} \mu_\Lambda^2 \varphi + \frac{1}{4!} \lambda_{1\Lambda} \varphi^2 + \lambda_{2\Lambda} \xi. \quad (21)$$

B. Functional Renormalization Group Equation

The functional RG equation in this system with $U(2) \times U(2)$ symmetry has the same form as the generic one (7) in the previous section. Thus, the functional RG equation in the LPA takes the following form (with $d = 3$):

$$\frac{\partial U_k(\varphi, \xi)}{\partial k} = K_d k^{d+1} \sum_i \frac{1}{E_i^2}, \quad (22)$$

where the energies in the denominator are for $i = \sigma, \vec{\pi}, \eta$, and \vec{a} , given with the mass eigenvalues obtained from the potential curvature. One might imagine that this straightforward procedure should work if U_k is given as an explicit function in terms of $\sigma, \vec{\pi}, \eta$, and \vec{a} . In fact, however, the $U(2) \times U(2)$ symmetry constrains the potential and U_k is a function of only two independent variables instead of four; that is, U_k is parametrized by φ and ξ only as exemplified in Eq. (21).

Below we will elucidate how to read off the expressions for the mass eigenvalues from the derivatives of $U_k(\varphi, \xi)$,

which requires a particular strategy for the calculation. Actually taking the second derivative on $U_k(\varphi, \xi)$ is just a simple manipulation. The most non-trivial part lies in the following: The resulting masses are easily expressed in terms of $\sigma, \vec{\pi}, \eta$, and \vec{a} , which must be converted into φ and ξ in the end.

We can simplify the problem a bit by observing that one field (σ in our case) acquires a non-vanishing expectation value and others have a vanishing expectation value and can be set to zero in the end. This means that we should take $\varphi \rightarrow \sigma^2$ and $\xi \rightarrow 0$ after writing down the functional RG equations. It is therefore a good truncation to keep the ξ -dependent term only up to the first few orders [42]:

$$U_k(\varphi, \xi) = V_k(\varphi) + W_k(\varphi) \xi + O(\xi^2). \quad (23)$$

In the present case we truncate the above expansion up to the linear order in ξ (where ξ is by definition of quartic order with respect to the meson field variables), so that our results cover at a minimum the same behavior that is captured in the perturbative ε -expansion. In other words, we can say that we have chosen an initial condition where the coefficient of the ξ^2 -order term is zero (as in Eq. (21)), and a truncation where it is set to remain zero throughout in the RG flow. This is the same-order truncation as the one used in [42, 43].

Let us demonstrate our strategy by taking an example of calculating M_σ^2 . The second derivative immediately leads to

$$\begin{aligned} M_\sigma^2 &= \frac{\partial^2 (V_k + W_k \xi)}{\partial \sigma^2} \\ &= 4\sigma^2 (V_k'' + W_k'' \xi) + 2(V_k' + W_k' \xi) + 2W_k \vec{a}^2 \\ &\quad + 8\sigma W_k' [\sigma(\eta^2 + \vec{a}^2) - \eta(\sigma\eta - \vec{\pi} \cdot \vec{a})]. \end{aligned} \quad (24)$$

It is highly non-trivial how to rewrite this expression for M_σ^2 into a form in terms of φ and ξ . We will do this by thinking of a particular situation where only σ and a^1 take a finite value. This is an almost unique choice for simplification; we can take $\vec{\pi}$ and η as small as we like, but \vec{a} is constrained by Eq. (20) for a given set of φ and ξ . Then we have

$$\varphi = \sigma^2 + (a^1)^2, \quad \xi = \sigma^2 (a^1)^2, \quad (25)$$

from which we can solve for σ and a^1 as

$$\sigma^2, (a^1)^2 = \frac{\varphi}{2} \pm \sqrt{\frac{\varphi^2}{4} - \xi}, \quad (26)$$

which can be expanded in terms of ξ into a form;

$$\sigma^2 = \varphi - \frac{\xi}{\varphi}, \quad (a^1)^2 = \frac{\xi}{\varphi}, \quad (27)$$

up to the linear order of ξ (higher-order terms are unnecessary in the $\xi \rightarrow 0$ limit). These expanded forms look singular at $\varphi \rightarrow 0$, but one should keep in mind that the expansion assumes $\varphi \gg \xi$ in Eq. (26) and one can always

choose ξ in such a way that ξ is small enough to satisfy this inequality. Therefore the singularity at $\varphi \rightarrow 0$ is only spurious, as we will check explicitly later.

Substituting these expressions into M_σ^2 we find

$$M_\sigma^2 = 4V_k'' \left(\varphi - \frac{\xi}{\varphi} \right) + 4W_k'' \varphi \xi + 2V_k' + 10W_k' \xi + 2W_k \frac{\xi}{\varphi}. \quad (28)$$

In the same way we can read the mass expressions off for other meson fields:

$$M_{\pi^1}^2 = M_\eta^2 = 2V_k' + 2W_k' \xi, \quad (29)$$

$$M_{\pi^2}^2 = M_{\pi^3}^2 = M_{\pi^1}^2 + 2W_k \frac{\xi}{\varphi}, \quad (30)$$

$$M_{a^1}^2 = M_{\pi^1}^2 + 4V_k'' \frac{\xi}{\varphi} + 8W_k' \xi + 2W_k \left(\varphi - \frac{\xi}{\varphi} \right), \quad (31)$$

$$M_{a^2}^2 = M_{a^3}^2 = M_{\pi^1}^2 + 2W_k \left(\varphi - \frac{\xi}{\varphi} \right). \quad (32)$$

We remark here that, if $U_k(\varphi, \xi)$ contains a term of order ξ^2 , the mass $M_{a^1}^2$ would have an extra term proportional to $\varphi \xi$, which is vanishing in the present case due to our choice of the initial condition and the truncation.

It is important to note that the mass matrix does not only have diagonal components but also off-diagonal ones which lead to a mixing between different fields. These off-diagonal components are given by

$$M_{\sigma-a^1}^2 = 4(V_k'' + W_k + W_k' \varphi) \sqrt{\xi}, \quad (33)$$

$$M_{\eta-\pi^1}^2 = 2W_k \sqrt{\xi}. \quad (34)$$

In order to make use of the simple expression for the functional RG equation in Eq. (22), we have to identify the eigenmodes $(\tilde{\sigma}, \tilde{a}^1)$ for the σ - a^1 part and $(\tilde{\eta}, \tilde{\pi}^1)$ for the η - π^1 part. It is not difficult to find the eigenvalues of the 2×2 matrix spanned in σ - a^1 space and the results are found to be

$$M_\sigma^2 = 4V_k'' \left(\varphi - \frac{\xi}{\varphi} \right) + 4W_k'' \varphi \xi + 2V_k' + 10W_k' \xi + 2W_k \frac{\xi}{\varphi} + \frac{8(V_k'' + W_k + W_k' \varphi)^2 \xi}{2V_k'' - W_k} \frac{\xi}{\varphi}, \quad (35)$$

$$M_{\tilde{a}^1}^2 = 4V_k'' \frac{\xi}{\varphi} + 2V_k' + 10W_k' \xi + 2W_k \left(\varphi - \frac{\xi}{\varphi} \right) - \frac{8(V_k'' + W_k + W_k' \varphi)^2 \xi}{2V_k'' - W_k} \frac{\xi}{\varphi}. \quad (36)$$

In the same way, regarding the η - π^1 mixing, we diagonalize the mass matrix, yielding

$$M_{\tilde{\eta}}^2 = 2V_k' + 2W_k' \xi + 2W_k \sqrt{\xi}, \quad (37)$$

$$M_{\tilde{\pi}^1}^2 = 2V_k' + 2W_k' \xi - 2W_k \sqrt{\xi}. \quad (38)$$

The remaining task is to decompose the functional RG equation into the one contributing to $V_k(\varphi)$ and the other

contributing to $W_k(\varphi)$. As seen from the LHS of Eq. (22), the part contributing to $W_k(\varphi)$ must come from terms proportional to ξ . (In the above the terms of $O(\sqrt{\xi})$ cancel between M_η^2 and $M_{\pi^1}^2$.) Thus, we should expand the RHS of Eq. (22) and identify the flow equations for $V_k(\varphi)$ and $W_k(\varphi)$ from the contributions of $O(\xi^0)$ and $O(\xi^1)$, respectively.

The $O(\xi^0)$ contribution is easy to derive from Eq. (22), that is,

$$\frac{\partial V_k}{\partial k} = K_d k^{d+1} \left(\frac{1}{E_\sigma^2} + \frac{4}{E_{\pi\eta}^2} + \frac{3}{E_a^2} \right), \quad (39)$$

where we define

$$E_\sigma^2 = k^2 + 2V_k' + 4V_k'' \varphi, \quad (40)$$

$$E_{\pi\eta}^2 = k^2 + 2V_k', \quad (41)$$

$$E_a^2 = k^2 + 2V_k' + 2W_k \varphi. \quad (42)$$

The calculations in the order $O(\xi^1)$ are rather complicated. After tedious but straightforward computations we finally obtain

$$\begin{aligned} \frac{\partial W_k}{\partial k} = & -K_d k^{d+1} \left\{ \frac{8W_k' + 4W_k \varphi^{-1}}{E_{\pi\eta}^4} - \frac{8W_k^2}{E_{\pi\eta}^6} \right. \\ & + \left[-4V_k'' \varphi^{-1} + 4W_k'' \varphi + 10W_k' + 2W_k \varphi^{-1} \right. \\ & \left. \left. + \frac{8(V_k'' + W_k + W_k' \varphi)^2}{2V_k'' - W_k} \varphi^{-1} \right] \frac{1}{E_\sigma^4} \right. \\ & + \left[4V_k'' \varphi^{-1} + 14W_k' - 6W_k \varphi^{-1} \right. \\ & \left. \left. - \frac{8(V_k'' + W_k + W_k' \varphi)^2}{2V_k'' - W_k} \varphi^{-1} \right] \frac{1}{E_a^4} \right\}. \quad (43) \end{aligned}$$

The above equations (39), (42), and (43) are our central results at the algebraic level. We emphasize that, thanks to the choice of the optimized IR regulator, these expressions no longer contain momentum integrals and are much simpler compared to those in earlier works. This also makes the connection to perturbative RG results more apparent.

Now let us make sure that Eq. (43) is not singular at $\varphi \rightarrow 0$. We see that the energy denominator becomes the same in all terms, i.e. $E_\sigma^2 = E_{\pi\eta}^2 = E_a^2$, as the limit $\varphi \rightarrow 0$ is taken. Then, we pick up the singular terms from the parentheses in the RHS of Eq. (43), whose coefficients amount to

$$4W_k + \left[-4V_k'' + 2W_k + \frac{8(V_k'' + W_k)^2}{2V_k'' - W_k} \right] + \left[4V_k'' - 6W_k - \frac{8(V_k'' + W_k)^2}{2V_k'' - W_k} \right] = 0, \quad (44)$$

where the first term is due to the part with $E_{\pi\eta}^4$, the second parenthesis to the part with E_σ^4 , and the last parenthesis to the part with E_a^4 in the functional RG equation (43).

C. Flow in Parameter Space

Let us check that our equations (39), (42), and (43) are consistent with the known results from the ε -expansion [5, 7]. To this end we expand the potential up to the fourth order or sixth order in terms of the fields:

$$V_k = \frac{1}{2}\mu_k^2\varphi + \frac{1}{4!}\lambda_{1k}\varphi^2 + \zeta_{1k}\varphi^3, \quad W_k = \lambda_{2k} + \zeta_{2k}\varphi, \quad (45)$$

where a constant offset of the potential energy is dropped. It should be noted that ξ is already of fourth order. For notational convenience, we will use λ_{1k} and λ_{2k} and will change to the couplings g_1 and g_2 only at the end to make a comparison with the ε -expansion results.

By expanding the flow equation in terms of φ , we can formulate the flow of the coupling constants (where we will set $\zeta_{1k} = \zeta_{2k} = 0$ and work up to the fourth order for the moment) as

$$\begin{aligned} \frac{\partial V_k}{\partial k} &= \frac{1}{2} \frac{\partial \mu_k^2}{\partial k} \varphi + \frac{1}{4!} \frac{\partial \lambda_{1k}}{\partial k} \varphi^2 \\ &= K_d k^{d+1} \left(\frac{8}{E^2} - \frac{5\lambda_{1k} + 18\lambda_{2k}}{3E^4} \varphi \right. \\ &\quad \left. + \frac{4\lambda_{1k}^2 + 18\lambda_{1k}\lambda_{2k} + 108\lambda_{2k}^2}{9E^6} \varphi^2 \right), \end{aligned} \quad (46)$$

where $E^2 = k^2 + \mu_k^2$. We also have

$$\frac{\partial W_k}{\partial k} = \frac{\partial \lambda_{2k}}{\partial k} = K_d k^{d+1} \frac{8\lambda_{1k}\lambda_{2k} + 16\lambda_{2k}^2}{E^6}. \quad (47)$$

We note that there is a cancellation which eliminates the terms proportional to φ^{-1} from the results, as we have already checked before. This allows us to easily decompose the flow equations into

$$\frac{\partial \mu_k^2}{\partial k} = -\frac{2K_d k^{d+1}}{3E^4} (5\lambda_{1k} + 18\lambda_{2k}), \quad (48)$$

$$\frac{\partial \lambda_{1k}}{\partial k} = \frac{16K_d k^{d+1}}{3E^6} (2\lambda_{1k}^2 + 9\lambda_{1k}\lambda_{2k} + 54\lambda_{2k}^2), \quad (49)$$

$$\frac{\partial \lambda_{2k}}{\partial k} = \frac{8K_d k^{d+1}}{E^6} (\lambda_{1k}\lambda_{2k} + 2\lambda_{2k}^2), \quad (50)$$

up to the fourth order for d dimensions. At this point, it is a simple task to convert the above into the ε -expansion results obtained by Pisarski and Wilczek [7]. We rescale the coupling constants in the following way (see also Eq. (19)):

$$\lambda_{1k} = 4! \frac{\pi^2}{3} \left(\bar{g}_1 + \frac{1}{2} \bar{g}_2 \right) k^{4-d}, \quad \lambda_{2k} = \frac{2\pi^2}{3} \bar{g}_2 k^{4-d}, \quad (51)$$

and use $\bar{\mu}_k^2 = k^{-2}\mu_k^2$ as previously defined. Then, after a short calculation, in $d = 4 - \varepsilon$ dimensions, we readily arrive at

$$k \frac{\partial \bar{g}_1}{\partial k} = -\varepsilon \bar{g}_1 + \frac{8}{3} \bar{g}_1^2 + \frac{8}{3} \bar{g}_1 \bar{g}_2 + \bar{g}_2^2, \quad (52)$$

$$k \frac{\partial \bar{g}_2}{\partial k} = -\varepsilon \bar{g}_2 + 2\bar{g}_1 \bar{g}_2 + \frac{4}{3} \bar{g}_2^2, \quad (53)$$

up to quadratic order in ε on the RHS, where we evaluated K_d at the expansion point $d = 4$ and used $K_4 = (32\pi^2)^{-1}$. This clearly shows that our calculations correctly reproduce the results in the ε -expansion in the leading order, as they should. One can prove that the flow with respect to \bar{g}_1 and \bar{g}_2 (with $\bar{\mu}_k = 0$) does not have any stable IR fixed point [7]. This is a reasonable but indirect argument that the phase transition should be a fluctuation-induced first order one [3]. It is highly non-trivial why the behavior of \bar{g}_1 and \bar{g}_2 is capable of describing a form of the potential which admits a first-order phase transition. Let us consider this question by taking account of the flow behavior of $\bar{\mu}_k^2$, which already goes beyond the ε -expansion (in which $\bar{\mu}_k^2 = 0$).

The set of equations (48), (49), and (50) is our convenient starting point to deal with the parameter flow because one can intuitively connect λ_{1k} and λ_{2k} to the shape of the potential; λ_{1k} is a coefficient of the quadratic term φ^2 (i.e. the quartic term σ^4). The flow equations for the dimensionless couplings in $d = 3$ dimensions, $\bar{\mu}_k^2$, $\bar{\lambda}_{1k}$, and $\bar{\lambda}_{2k}$, are

$$k \frac{\partial \bar{\mu}_k^2}{\partial k} = -2\bar{\mu}_k^2 - \frac{1}{9\pi^2(1 + \bar{\mu}_k^2)^2} (5\bar{\lambda}_{1k} + 18\bar{\lambda}_{2k}), \quad (54)$$

$$\begin{aligned} k \frac{\partial \bar{\lambda}_{1k}}{\partial k} &= -\bar{\lambda}_{1k} \\ &\quad + \frac{8}{9\pi^2(1 + \bar{\mu}_k^2)^3} (2\bar{\lambda}_{1k}^2 + 9\bar{\lambda}_{1k}\bar{\lambda}_{2k} + 54\bar{\lambda}_{2k}^2), \end{aligned} \quad (55)$$

$$k \frac{\partial \bar{\lambda}_{2k}}{\partial k} = -\bar{\lambda}_{2k} + \frac{4}{3\pi^2(1 + \bar{\mu}_k^2)^3} (\bar{\lambda}_{1k}\bar{\lambda}_{2k} + 2\bar{\lambda}_{2k}^2). \quad (56)$$

In the same way it is tedious but straightforward to write down the differential equations including sixth-order couplings ζ_{1k} and ζ_{2k} . The expressions are easily derived from Eqs. (39) and (43) and they are too lengthy to display here, so we shall give their explicit forms in the Appendix.

We solve these differential equations numerically. The RHS of these equations has no explicit dependence on the scale k and the LHS can be rewritten as $k\partial/\partial k = \partial/\partial t$ using $t \equiv \ln(k/\Lambda)$, so that we can describe the RG flow in terms of this variable. We numerically trace the running of these couplings from $t = 0$ to $t = -2.3$ (i.e. $k = 0.1\Lambda$) to determine the flow diagram, using the fourth-order Runge-Kutta method. We used an adaptive step size ($< 10^{-4}$) so that no numerical instability occurs. [In later discussions we will use the fifth-order Runge-Kutta-Fehlberg (4,5) (RKF45) method to solve the functional equations. In the present case, where the partial differential equations are relatively simple, the fourth-order method is sufficient.]

The case with $\bar{\lambda}_{2\Lambda} = 0$ (Fig. 1): Let us begin with a simple case. We see that $\bar{\lambda}_{2k} = 0$ is a solution of Eq. (56). If we start the RG flow with the initial condition $\bar{\lambda}_{2\Lambda} = 0$, this means that $\bar{\lambda}_{2k}$ remains zero for any k throughout the flow and Eqs. (54) and (55) determine the evolution of $\bar{\mu}_k^2$ and $\bar{\lambda}_{1k}$ with changing k (up to the fourth-order of

the Taylor expansion). In this case with $\bar{\lambda}_{2k} = 0$ the flow equations are reduced to those in the $O(8)$ -symmetric scalar theory. It is easy to make sure that we can also reproduce the well-known results from the ε -expansion by setting $\bar{\lambda}_{2k} = 0$ and using $K_4 = (32\pi^2)^{-1}$ in the above expressions. To go to the next-to-leading order in the ε -expansion one must go beyond the local potential approximation, as done in the derivative expansion [46, 78] or in the so-called BMW approximation [79], which is beyond the scope of our present approach.

Using Eqs. (54) and (55) with $\bar{\lambda}_{2k} = 0$, we plot the RG flow to obtain Fig. 1. We find an IR fixed point at

$$\begin{aligned} \bar{\mu}_*^2 &= -\frac{5}{37} \approx -0.135, \\ \bar{\lambda}_{1*} &= \frac{9\pi^2}{16} \left(\frac{32}{37}\right)^3 \approx 3.59. \end{aligned} \quad (57)$$

We find indeed in Fig. 1 a fixed point corresponding to the second-order phase transition at these values of the couplings. It is obvious from Fig. 1 that there is no RG trajectory flowing from the $(\bar{\mu}_k^2 < 0, \bar{\lambda}_{1k} > 0)$ region into the $(\bar{\mu}_k^2 > 0, \bar{\lambda}_{1k} < 0)$ region. Thus it is not possible to arrive at a fluctuation-induced first-order phase transition as long as the initial $\bar{\lambda}_{2\Lambda}$ is chosen to be zero. We see that such a flow which would favor a fluctuation-induced first-order transition is prevented by the presence of the UV fixed point at the origin from which the flow emerges.

The case with $\bar{\lambda}_{2\Lambda} \neq 0$ (Figs. 4, 5, 6): Now we proceed to the case with a finite λ_{2k} . Interestingly enough, the flow pattern changes drastically once $\bar{\lambda}_{2\Lambda}$ deviates from zero. Then we have to analyze the flow pattern as a function of $\bar{\mu}_k^2$, $\bar{\lambda}_{1k}$, and $\bar{\lambda}_{2k}$. To visualize the flow pattern, we solve Eqs. (54), (55), and (56) for a particular initial condition with a certain choice of $\bar{\lambda}_{2\Lambda}$, and investigate the destination of the flow in the $\bar{\mu}_k^2$ - $\bar{\lambda}_{1k}$ plane. As we have already elucidated in Fig. 2 in the $O(8)$ case and also in Figs. 4, 5, and 6, we can classify the parameter regions according to qualitative features of the potential form;

$$\begin{aligned} \bar{\mu}_k^2 < 0 \text{ and } \bar{\lambda}_{1k} > 0 &\rightarrow \text{Symmetry-broken} \\ \bar{\mu}_k^2 > 0 \text{ and } \bar{\lambda}_{1k} > 0 &\rightarrow \text{Symmetric} \\ \bar{\mu}_k^2 > 0 \text{ and } \bar{\lambda}_{1k} < 0 &\rightarrow \text{Necessary for Double-well} \end{aligned}$$

as $k \rightarrow 0$.

We have already discussed our results in Sec. II. As a final remark in this subsection, we point out an interesting consequence from the flow equations.

From an analysis of the flow equations (54), (55), and (56) we can indeed confirm that in this approximation no fixed point with $\lambda_{2k} \neq 0$ exists in $d = 3$ dimensions, and in the presence of a non-zero coupling λ_{2k} a second-order phase transition associated with this fixed point cannot be accommodated.

To see this, the fixed point $(\bar{\mu}_*^2, \bar{\lambda}_{1*}, \bar{\lambda}_{2*})$ is located by imposing the condition that the RHS's of Eqs. (54), (55), and (56) vanish. For $\bar{\lambda}_{2*} \neq 0$, the fixed point condition

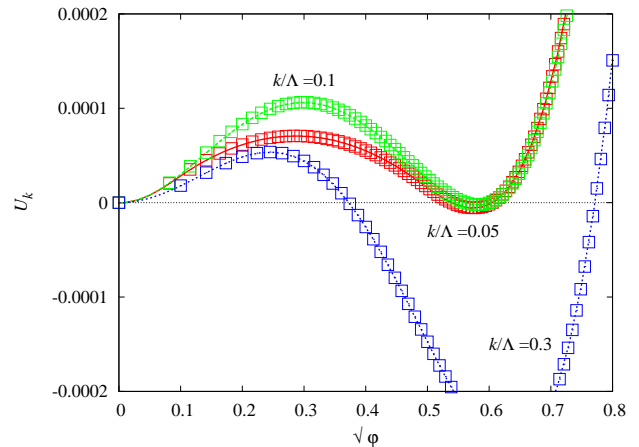


FIG. 7. Evolution of the form of the potential with decreasing k/Λ in the case with $\lambda_{2\Lambda} = 0.4$. The solid curves represent the results from our grid method (see the text for details) and the squares represent the results obtained in the method formulated in [80]. The potential is given as a function of $\sqrt{\varphi}$. The initial parameters are chosen as $\mu_\Lambda^2 = -0.05$ and $\lambda_{1\Lambda} = 0.35$.

can be simplified and the resulting system of three equations for the three couplings $\bar{\mu}_*^2$, $\bar{\lambda}_{1*}$, and $\bar{\lambda}_{2*}$ can be solved analytically. We find that for $d = 3$ no solutions for real values of the couplings exist (that is, $\bar{\mu}_*^2$, $\bar{\lambda}_{1*}$, and $\bar{\lambda}_{2*}$ are all complex then), and that hence the RG flow in this approximation does not admit a second-order phase transition.

D. Functional Solution

Without an evaluation of the higher-order terms we cannot locate exactly where the fluctuation-induced first-order phase transition takes place on Figs. 4, 5, and 6. Nevertheless, it is clear that the second-order critical line is overridden by the region which satisfies the condition for a double-well potential as the initial value for $\lambda_{2\Lambda}$ grows (see particularly Figs. 1 and 4).

We can check if the analytical study in the previous subsection is qualitatively correct by looking at the full functional solution obtained with the grid method. Since there is no scaling property expected in the case of the fluctuation-induced first-order phase transition, we plot the results in terms of unscaled variables (made dimensionless not with k but by the UV scale Λ). We give the numerical values for μ_k^2 , λ_{1k} , and λ_{2k} in units of Λ and we omit Λ hereafter.

In the numerical calculations, we used a simple formulation for the grid method. We first discretize the function $U_k(\varphi)$ in terms of $\sigma = \sqrt{\varphi}$ instead of φ , since we are interested in the characteristic form of the effective potential in the vicinity of $\varphi \sim 0$ or $\sigma \sim 0$. It is thus more suitable to use σ to attain more resolution in the small- φ region. Our mesh size is $\Delta\sigma = 10^{-2}$ and the

mesh spans the interval between $\sigma = \pm 2$. The singularity in the flow equations at $\sigma = 0$ is only spurious due to cancellation as we have checked. In the numerical calculation one should remove this singularity analytically or discretize the fields not to hit the origin. We here took the latter, i.e. we choose the support points such that the origin is not included; $\sigma_i = \Delta\sigma(i + 0.5)$ with i ranging from -200 to 199 . To evaluate the derivatives U'_k and U''_k we used the 7-point formula. At the boundaries, where we cannot take 7 points (i.e. 3 adjacent sites from the point where the derivatives are evaluated), we used the 5-point formula and the 3-point formula, and eventually at the very end we approximately used the next-site value. These procedures enhance numerical errors locally near the edges, but if the edges are sufficiently far from the small- φ region of our interest, those errors do not influence the results. The step size Δk is an adaptive variable so that the computation proceeds without numerical instability. Typically Δk is less than 10^{-4} . Then we found no instability in the fourth-order Runge-Kutta method. In summary, after discretization we treat the function $U_k(\varphi)$ as an array labelled by site number i and then proceed as follows:

1. Choose an initial value of $k = \Lambda$ and fix the potential parameters μ_Λ , $\lambda_{1\Lambda}$, and $\lambda_{2\Lambda}$ which also determines the initial configuration of the array for $V_\Lambda(\sigma)$ and $W_\Lambda(\sigma)$ (where $\sigma = \sqrt{\varphi}$).
2. Evaluate the RHS of Eqs. (39) and (43) using $V_k(\sigma)$ and $W_k(\sigma)$, and the numerical derivatives. Update the potential from $V_k(\sigma)$ and $W_k(\sigma)$ down to $V_{k-\Delta k}(\sigma)$ and $W_{k-\Delta k}(\sigma)$ with the Runge-Kutta method.
3. Iterate the above calculation until the scale k reaches zero or a sufficiently small value, so that the full effective potential $V_0(\sigma)$ and $W_0(\sigma)$ results at the end from the functional RG flow.

Such a discretization scheme may look very simple compared to more sophisticated processes such as the one proposed in [80], which has actually been used in the earlier works [42, 43]. In this method U_k and U'_k are solved for by the evolution equations and U''_k and U'''_k are determined by the matching condition. While the idea sounds very different from the simple numerical derivatives that we used, the matching condition leads in effect to a natural generalization of the formula for the numerical differentiation. The accuracy is likely better than that of the 7-point formula. In addition, for the method of [80], usually the RKF45 method (fifth-order Runge-Kutta method with the fourth-order embedded for the error control) is used. This sophisticated method is very powerful, but at the same time, it is difficult to apply it to solve a flow equation with many terms, such as Eq. (43).

We prefer to use the former simpler method as long as it works and we do not need high precision data. In fact we have solved the RG equations making use of both

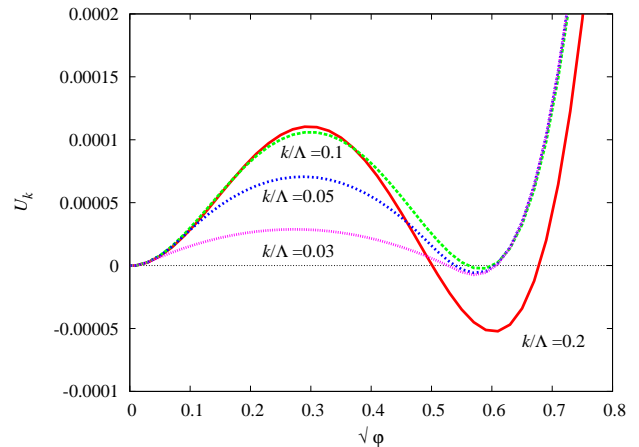


FIG. 8. Evolution of the form of the potential in the region with $k/\Lambda < 0.2$ in the case with $\lambda_{2\Lambda} = 0.4$ as k/Λ decreases. At $k/\Lambda = 1$ the initial parameters are chosen as $\mu_\Lambda^2 = -0.05$ and $\lambda_{1\Lambda} = 0.35$.

the simple and sophisticated method, and we present a quantitative comparison in Fig. 7. We clearly see that the potential exhibits a double-well form as a result of fluctuations and the deviation by two methods is not visible in the figure. We can conclude that our method is good enough for our purpose.

We have already discussed our central results in Sec. II and so we do not reiterate the discussion here. For the rest of this subsection we mention on some notable features in the potential evolution.

Figures 7 and 8 show the evolution of the shape of the potential in the case of $\lambda_{2\Lambda} = 0.4$ starting with the initial condition $\mu_\Lambda^2 = -0.05$ and $\lambda_{1\Lambda} = 0.35$, which is almost at the first-order phase transition point (as indicated by the solid line in Figs. 4 and 5). We stopped the evolution at $k/\Lambda = 0.1$, which is legitimate because the effective potential becomes convex when k/Λ goes to zero and the double-well shape of the potential is less manifest [81]. Here this happens below $k/\Lambda \sim 0.1$, as shown in Fig. 8. We can clearly see in Fig. 8 that the location of the minima does not change for $k/\Lambda < 0.1$, although the bump of the potential is becoming flat with smaller k/Λ . This is completely consistent with the observation in Ref. [42] and justifies our prescription to stop the RG evolution at $k/\Lambda = 0.1$ in order to judge if the potential has a double-well shape. Even though we choose the step size Δk as an adaptive variable, moreover, our algorithm loses stability at $k/\Lambda \sim 0.02$ and cannot reach the completely flat shape. We observed the same behavior even using the matching method with the RKF45 method. Probably the implicit method (i.e. Lax method) might cure this problem. In any case, since our aim is simply to determine the transition line on the phase diagram shown in Figs. 4 and 5, there is no practical need to require the potential form at $k/\Lambda < 0.1$.

The first-order phase transition occurs with varying μ_Λ^2 and/or $\lambda_{1\Lambda}$ for a given $\lambda_{2\Lambda}$. Let us fix μ_Λ^2 at -0.05

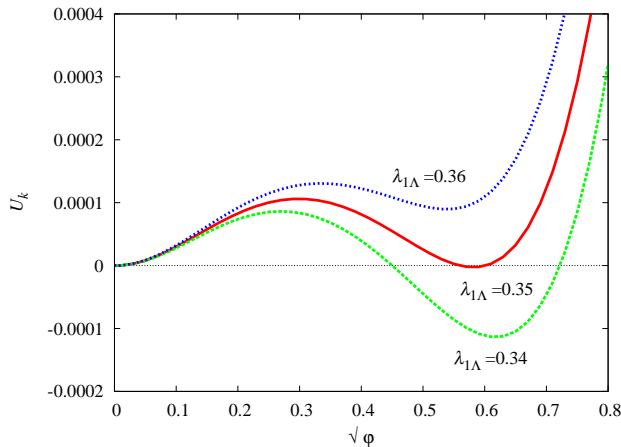


FIG. 9. Change of the form of the potential as the initial value $\lambda_{1\Lambda}$ changes around 0.35. All results for the potential are given at fixed $k/\Lambda = 0.1$. Other initial parameters are all chosen to be the same as in Fig. 7.

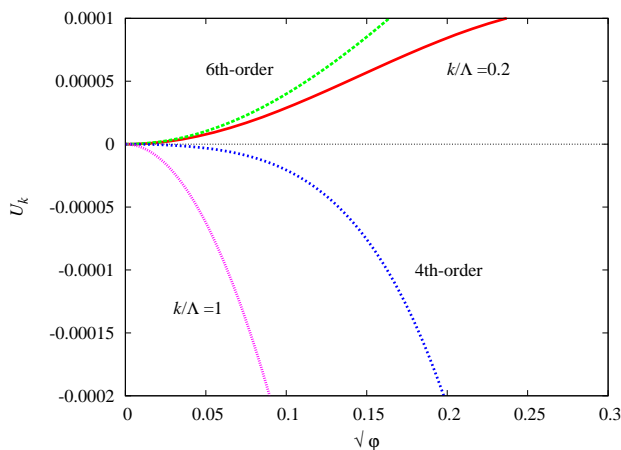


FIG. 10. Comparison between the full effective potentials at $k/\Lambda = 0.2$ and the expanded results from the Taylor expansion up to fourth order and sixth order. The effective potential at $k/\Lambda = 1$ is presented for reference.

here and change $\lambda_{1\Lambda}$ to see how the first-order transition arises. Our results are depicted in Fig. 9. Again, we have stopped the evolution at $k/\Lambda = 0.1$, which is sufficient to find a first-order phase transition. It is obvious that there is a peculiar change of the shape of the potential which is associated with the first-order phase transition from $\lambda_{1\Lambda} = 0.34$ to 0.36. More precisely, we can locate the transition point by detecting the second minimum height and using the midpoint method for $\lambda_{1\Lambda}$, which leads to a critical value of $\lambda_{1\Lambda} = 0.3509$. We picked just one example of particular values of μ_Λ^2 but can repeat the same procedure with different parameters to find a first-order phase transition line as indicated in Figs. 4, 5, and 6.

Finally let us discuss the comparison between the full functional solutions and the Taylor expansion results. We

present Fig. 10 to show the expanded results according to Eq. (45) together with the outputs from the grid calculation. It may be surprising at first glance that the curvature at $\sqrt{\varphi} \simeq 0$ has such large deviations from the fourth-order results and the sixth-order or full grid results. We observe that the agreement in the curvature stays good as long as k/Λ is not too small ($k/\Lambda \sim 0.5$ for instance), for which the curvature is still negative. Even though the Taylor expansion in terms of the field φ should in principle work well in the small- φ region, the fourth-order expansion is not good enough to capture the first-order phase transition quantitatively. We can see that the agreement in the curvature is significantly improved by proceeding to the sixth-order expansion, though the agreement in the quartic coefficient (i.e. λ_{1k}) seems to be poor, which might be improved with inclusion of further higher-order contributions.

V. CONCLUSIONS

We have applied the functional RG technique in the form of Wetterich's flow equation to an analysis of a scalar theory with $U(2) \times U(2)$ symmetry. We have been able to recover the perturbative results by means of expansion in terms of the field, which also encompasses the standard ε -expansion results [7]. The choice of a suitable regulator function and the resulting simple form of the RG flow equations make this connection apparent. Going beyond a perturbative expansion in small couplings, we have further used the functional RG flow equation in the local potential approximation to study the emergence of a first-order phase transition. To this end, we have discretized the effective potential on a mesh grid to obtain the global shape of the potential for a set of choices for the initial conditions. Our results confirm those of earlier studies [42, 43].

In the $U(2) \times U(2)$ scalar theory there are two fourth-order couplings – λ_{1k} appearing in the quartic coefficient in the effective potential and λ_{2k} which has no counterpart in the $O(N)$ theory – in addition to the curvature μ_k^2 . We have found that the second-order critical line in the $\bar{\mu}_k^2$ - $\bar{\lambda}_{1k}$ plane is gradually overridden by the first-order phase transition as the initial value $\bar{\lambda}_{2\Lambda}$ starts to differ from zero. We find analytically that no fixed point associated with a second-order transition exists for $d = 3$ and $\bar{\lambda}_{2k} \neq 0$ in our approximation which is perturbative but beyond the ε -expansion.

In view of the expanded potential, a double-well shape of the potential is possible in the region $\bar{\mu}_\Lambda^2 > 0$ and $\bar{\lambda}_{1\Lambda} < 0$, which would admit a first-order transition if the potential is stabilized by higher-order terms, which we investigated up to the sixth-order expansion. We note that a similar analysis has been performed in Ref. [10] up to the eighth-order expansion for the Coleman-Weinberg potential and our results are qualitatively consistent with those of Ref. [10]. From the flow diagram we learn that one way to understand the fluctuation-induced first-order

phase transition is that this first-order phase transition at the tree level with $\bar{\mu}_\Lambda^2 > 0$ and $\bar{\lambda}_{1\Lambda} < 0$ penetrates into other (physical) parameter regions for $\bar{\lambda}_{2\Lambda} \neq 0$. This is an interesting point of view and gives an intuitive insight into the emergence of a fluctuation-induced first-order phase transition.

Regarding the application to QCD physics, it would be intriguing to study the chiral phase transition with both the meson fluctuations [69, 70] and the effective restoration of $U(1)_A$ symmetry taken into account. So far, for example, the so-called Columbia diagram in the mass plane of light and heavy quarks has been investigated as a function of the $U(1)_A$ -breaking strength [64, 67]. The possibility of the fluctuation-induced first-order phase transition, however, has not yet been considered because the model study was at the mean-field level. The present work gives a theoretical framework necessary for such investigations in the future.

ACKNOWLEDGMENTS

We thank Jean-Paul Blaizot, Jan Pawłowski, and Jens Braun for useful discussions. K. F. was supported by

Grant-in-Aid for Young Scientists B (No. 20740134) and also supported in part by Yukawa International Program for Quark Hadron Sciences. K. K. was supported by Grant-in-Aid for JSPS Fellows (No. 22-3671). B. K. acknowledges support by the Research Cluster ‘‘Structure and Origin of the Universe’’.

Appendix A: FLOW EQUATIONS IN THE SIXTH-ORDER TAYLOR EXPANSION

Here we list a set of differential equations involving the sixth-order Taylor coefficients ζ_1 and ζ_2 . We note that Eq. (48) for μ_k^2 has no modification. Equations (49) and (50) are replaced, respectively, by

$$\frac{\partial \lambda_{1k}}{\partial k} = \frac{16K_d k^{d+1}}{3E^6} [2\lambda_{1k}^2 + 9\lambda_{1k}\lambda_{2k} + 54\lambda_{2k}^2 - 27E^2(12\zeta_{1k} + \zeta_{2k})], \quad (\text{A1})$$

$$\frac{\partial \lambda_{2k}}{\partial k} = \frac{8K_d k^{d+1}}{E^6} (\lambda_{1k}\lambda_{2k} + 2\lambda_{2k}^2 - 4\zeta_{2k}E^2), \quad (\text{A2})$$

which are reduced to Eqs. (49) and (50) for $\zeta_{1k} = \zeta_{2k} = 0$. The differential equations for ζ_{1k} and ζ_{2k} are

$$\frac{\partial \zeta_{1k}}{\partial k} = -\frac{K_d k^{d+1}}{108E^8} \{17\lambda_{1k}^3 + 54\lambda_{1k}^2\lambda_{2k} + 648\lambda_{1k}\lambda_{2k}^2 + 2592\lambda_{2k}^3 - 216E^2[2\zeta_{1k}(11\lambda_{1k} + 18\lambda_{2k}) + \zeta_{2k}(\lambda_{1k} + 12\lambda_{2k})]\}, \quad (\text{A3})$$

$$\frac{\partial \zeta_{2k}}{\partial k} = -\frac{4K_d k^{d+1}}{3E^8} \{3\lambda_{2k}(2\lambda_{1k}^2 + 11\lambda_{1k}\lambda_{2k} + 6\lambda_{2k}^2) - E^2[432\zeta_{1k}\lambda_{2k} + \zeta_{2k}(23\lambda_{1k} + 114\lambda_{2k})]\}, \quad (\text{A4})$$

which were used to obtain the sixth-order results shown

in Figs. 5, 6, and 10.

-
- [1] S. R. Coleman and E. J. Weinberg, Phys. Rev. D **7**, 1888 (1973).
 - [2] B. I. Halperin, T. C. Lubensky and S. K. Ma, Phys. Rev. Lett. **32**, 292 (1974).
 - [3] P. Bak, S. Krinsky and D. Mukamel, Phys. Rev. Lett. **36**, 52 (1976).
 - [4] A. J. Paterson, Nucl. Phys. B **190**, 188 (1981).
 - [5] R. D. Pisarski and D. L. Stein, Phys. Rev. B **23**, 3549 (1981).
 - [6] H. H. Iacobson and D. J. Amit, Annals Phys. **133**, 57 (1981).
 - [7] R. D. Pisarski and F. Wilczek, Phys. Rev. D **29**, 338 (1984).
 - [8] S. Bornholdt, N. Tetradis and C. Wetterich, Phys. Lett. B **348**, 89 (1995).
 - [9] M. G. Alford, J. March-Russell, Nucl. Phys. **B417**, 527-552 (1994).
 - [10] D. Litim, C. Wetterich and N. Tetradis, Mod. Phys. Lett. A **12**, 2287 (1997).
 - [11] D. F. Litim, Phys. Lett. B **393**, 103 (1997).
 - [12] G. Baym and G. Grinstein, Phys. Rev. D **15**, 2897 (1977).
 - [13] J. B. Kogut, M. Snow and M. Stone, Nucl. Phys. B **200**, 211 (1982).
 - [14] G. Amelino-Camelia and S. Y. Pi, Phys. Rev. D **47**, 2356 (1993).
 - [15] S. Chiku and T. Hatsuda, Phys. Rev. D **58**, 076001 (1998).
 - [16] D. Roder, J. Ruppert and D. H. Rischke, Nucl. Phys. A **775**, 127 (2006).
 - [17] F. Cooper, J. F. Dawson and B. Mihaila, Phys. Rev. D **71**, 096003 (2005).
 - [18] J. C. Le Guillou and J. Zinn-Justin, Phys. Rev. Lett. **39**, 95 (1977); R. Guida and J. Zinn-Justin, J. Phys. A **31**, 8103 (1998).
 - [19] B. J. Schaefer and H. J. Pirner, Nucl. Phys. A **660**, 439 (1999).
 - [20] O. Bohr, B. J. Schaefer and J. Wambach, Int. J. Mod. Phys. A **16**, 3823 (2001).

- [21] J. D. Shafer and J. R. Shepard, Phys. Rev. D **67**, 085025 (2003).
- [22] J. P. Blaizot, A. Ipp, R. Mendez-Galain and N. Wschebor, Nucl. Phys. A **784**, 376 (2007).
- [23] F. Parisen Toldin, A. Pelissetto and E. Vicari, JHEP **0307**, 029 (2003).
- [24] J. Braun and B. Klein, Phys. Rev. D **77**, 096008 (2008); Eur. Phys. J. C **63**, 443 (2009).
- [25] For reviews, see; B. Svetitsky, Phys. Rept. **132**, 1 (1986); T. Hatsuda and T. Kunihiro, Phys. Rept. **247**, 221 (1994); H. Meyer-Ortmanns, Rev. Mod. Phys. **68**, 473 (1996); D. H. Rischke, Prog. Part. Nucl. Phys. **52**, 197 (2004); C. DeTar and U. M. Heller, Eur. Phys. J. A **41**, 405 (2009); K. Fukushima, T. Hatsuda, Rept. Prog. Phys. **74**, 014001 (2011).
- [26] F. Wilczek, Int. J. Mod. Phys. A **7**, 3911 (1992) [Erratum-ibid. A **7**, 6951 (1992)].
- [27] Y. Nambu and G. Jona-Lasinio, Phys. Rev. **122**, 345 (1961); Phys. Rev. **124**, 246 (1961).
- [28] M. Gell-Mann and M. Levy, Nuovo Cim. **16**, 705 (1960).
- [29] T. Appelquist and R. D. Pisarski, Phys. Rev. D **23**, 2305 (1981).
- [30] D. J. Gross, R. D. Pisarski and L. G. Yaffe, Rev. Mod. Phys. **53**, 43 (1981).
- [31] E. V. Shuryak, Comments Nucl. Part. Phys. **21**, 235 (1994).
- [32] T. Schäfer, Phys. Rev. D **65**, 094033 (2002).
- [33] K. G. Wilson, Phys. Rev. B **4**, 3174 (1971); Phys. Rev. B **4**, 3184 (1971); F. J. Wegner and A. Houghton, Phys. Rev. A **8**, 401 (1973).
- [34] K. G. Wilson and M. E. Fisher, Phys. Rev. Lett. **28**, 240 (1972).
- [35] K. G. Wilson and J. B. Kogut, Phys. Rept. **12**, 75 (1974).
- [36] H. Yamagishi, Phys. Rev. D **23**, 1880 (1981).
- [37] P. Calabrese, A. Pelissetto and E. Vicari, Phys. Rev. B **67**, 054505 (2003).
- [38] A. Butti, A. Pelissetto and E. Vicari, JHEP **0308**, 029 (2003).
- [39] E. Vicari, PoS **LAT2007**, 023 (2007).
- [40] D. U. Jungnickel and C. Wetterich, Phys. Rev. D **53**, 5142 (1996).
- [41] J. Berges, N. Tetradis and C. Wetterich, Phys. Rev. Lett. **77**, 873 (1996).
- [42] J. Berges and C. Wetterich, Nucl. Phys. B **487**, 675 (1997).
- [43] J. Berges, N. Tetradis and C. Wetterich, Phys. Lett. B **393**, 387 (1997).
- [44] C. Wetterich, Phys. Lett. B **301**, 90 (1993).
- [45] J. Berges, arXiv:hep-ph/9902419.
- [46] J. Berges, N. Tetradis and C. Wetterich, Phys. Rept. **363**, 223 (2002).
- [47] A. Ali Khan *et al.* [CP-PACS Collaboration], Phys. Rev. D **63**, 034502 (2001); F. Karsch, E. Laermann and C. Schmidt, Phys. Lett. B **520**, 41 (2001); M. D'Elia, A. Di Giacomo and C. Pica, Phys. Rev. D **72**, 114510 (2005); Y. Aoki, G. Endrodi, Z. Fodor, S. D. Katz and K. K. Szabo, Nature **443**, 675 (2006); Y. Aoki, Z. Fodor, S. D. Katz and K. K. Szabo, Phys. Lett. B **643**, 46 (2006); Y. Aoki, S. Borsanyi, S. Durr, Z. Fodor, S. D. Katz, S. Krieg and K. K. Szabo, JHEP **0906**, 088 (2009); S. Ejiri *et al.*, Phys. Rev. D **80**, 094505 (2009); F. Karsch, arXiv:1007.2393 [hep-lat].
- [48] B. Bergerhoff, F. Freire, D. Litim, S. Lola and C. Wetterich, Phys. Rev. B **53**, 5734 (1996); B. Bergerhoff, D. Litim, S. Lola and C. Wetterich, Int. J. Mod. Phys. A **11** (1996) 4273.
- [49] H. Gies and C. Wetterich, Phys. Rev. D **69**, 025001 (2004).
- [50] J. Braun, Eur. Phys. J. C **64**, 459 (2009).
- [51] R. Alkofer, C. S. Fischer and R. Williams, Eur. Phys. J. A **38**, 53 (2008); C. S. Fischer and R. Williams, Phys. Rev. D **78**, 074006 (2008).
- [52] D. F. Litim and J. M. Pawłowski, arXiv:hep-th/9901063.
- [53] C. Bagnuls and C. Bervillier, Phys. Rept. **348**, 91 (2001).
- [54] J. Polonyi, Central Eur. J. Phys. **1**, 1 (2003).
- [55] B. Delamotte, D. Mouhanna and M. Tissier, Phys. Rev. B **69**, 134413 (2004).
- [56] J. M. Pawłowski, Annals Phys. **322**, 2831 (2007).
- [57] H. Gies, arXiv:hep-ph/0611146.
- [58] B. Delamotte, arXiv:cond-mat/0702365.
- [59] H. Sonoda, arXiv:0710.1662 [hep-th].
- [60] O. J. Rosten, arXiv:1003.1366 [hep-th].
- [61] T. Papenbrock and C. Wetterich, Z. Phys. C **65**, 519 (1995).
- [62] D. F. Litim and J. M. Pawłowski, Phys. Rev. D **66**, 025030 (2002).
- [63] Y. Shen, Phys. Lett. B **315**, 146 (1993).
- [64] K. Fukushima, Phys. Lett. B **591**, 277 (2004); Phys. Rev. D **77**, 114028 (2008) [Erratum-ibid. D **78**, 039902 (2008)].
- [65] C. Ratti, M. A. Thaler and W. Weise, Phys. Rev. D **73**, 014019 (2006).
- [66] B.-J. Schaefer, J. M. Pawłowski and J. Wambach, Phys. Rev. D **76**, 074023 (2007).
- [67] W. J. Fu, Z. Zhang and Y. X. Liu, Phys. Rev. D **77**, 014006 (2008).
- [68] M. Ciminale, R. Gatto, N. D. Ippolito, G. Nardulli and M. Ruggieri, Phys. Rev. D **77**, 054023 (2008).
- [69] B.-J. Schaefer and J. Wambach, Nucl. Phys. A **757**, 479 (2005); Phys. Rev. D **75**, 085015 (2007); B.-J. Schaefer, M. Wagner and J. Wambach, Phys. Rev. D **81**, 074013 (2010); T. K. Herbst, J. M. Pawłowski, B.-J. Schaefer, Phys. Lett. **B696**, 58-67 (2011); F. Karsch, B.-J. Schaefer, M. Wagner and J. Wambach, arXiv:1009.5211 [hep-ph].
- [70] E. Nakano, B.-J. Schaefer, B. Stokic, B. Friman and K. Redlich, Phys. Lett. B **682**, 401 (2010); V. Skokov, B. Friman, E. Nakano, K. Redlich and B.-J. Schaefer, Phys. Rev. D **82**, 034029 (2010); V. Skokov, B. Friman and K. Redlich, arXiv:1008.4570 [hep-ph].
- [71] J. Braun, B. Klein, H. J. Pirner and A. H. Rezaeian, Phys. Rev. D **73**, 074010 (2006); J. Braun, B. Klein and P. Piasecki, arXiv:1008.2155 [hep-ph].
- [72] T. Sano, H. Fujii and M. Ohtani, Phys. Rev. D **80**, 034007 (2009); H. Fujii and T. Sano, arXiv:1009.5977 [hep-ph].
- [73] D. F. Litim, Phys. Lett. B **486**, 92 (2000).
- [74] D. F. Litim, Phys. Rev. D **64**, 105007 (2001); Nucl. Phys. B **631**, 128 (2002).
- [75] D. F. Litim, JHEP **0507**, 005 (2005); C. Bervillier, A. Juttner and D. F. Litim, Nucl. Phys. B **783**, 213 (2007).
- [76] D. F. Litim and J. M. Pawłowski, JHEP **0611**, 026 (2006).
- [77] J. Braun, K. Schwenzer and H. J. Pirner, Phys. Rev. D **70**, 085016 (2004).
- [78] D. F. Litim, JHEP **0111**, 059 (2001); D. F. Litim and D. Zappala, arXiv:1009.1948 [hep-th].

- [79] J. P. Blaizot, R. Mendez-Galain and N. Wschebor, Phys. Lett. B **632**, 571 (2006); Phys. Rev. E **74**, 051116 (2006); Phys. Rev. E **74**, 051117 (2006); F. Benitez, J. P. Blaizot, H. Chate, B. Delamotte, R. Mendez-Galain and N. Wschebor, Phys. Rev. E **80**, 030103 (2009).
- [80] J. A. Adams, J. Berges, S. Bornholdt, F. Freire, N. Tetradis and C. Wetterich, Mod. Phys. Lett. A **10**, 2367 (1995).
- [81] A. Ringwald and C. Wetterich, Nucl. Phys. B **334**, 506 (1990); N. Tetradis and C. Wetterich, Nucl. Phys. B **383**, 197 (1992).